11º Congresso Brasileiro de Engenharia de Fabricação
24 a 26 de maio de 2021, Curitiba, PR, Brasil

SMART DRILLING: MATERIAL IDENTIFICATION USING SPECIFIC FORCE MAP

Maria Clara Coimbra Gonçalves
Gilmar Ferreira Batalha
USP - Universidade de São Paulo, São Paulo, Brazil
mclara.coimbra@usp.br
Anna Carla Araujo
Yann Landon
Institut Clément Ader (ICA), Université de Toulouse, CNRS/INSA/ISAE/Mines Albi/UPS, Toulouse, France
araujo@insa-toulouse.fr
yann.landon@univ-tlse3.fr

Abstract. *Stacks materials are frequently applied in aeronautical industries due to its great combination properties. Although, as per different machinabilities, choosing the cutting parameters for drilling stacks is far from simple. Usually, in industries, the machining parameters are set to suit the most hard to machine material in a stack, which increases the cutting time and productivity. Smart machining techniques contribute to the development of drilling stacks materials by adapting the parameters to the identified material. The goal in the present work is to create a map for identification based on the specific force analysis using two metallic materials: aluminum and titanium alloys, often found in aeronautic stacks. The resultant map shows distinct regions for these materials proving it could be applied to use on smart drilling techniques.*

Keywords: *Machining. Smart drilling. Stack materials. Titanium. Aluminum.*

1. INTRODUCTION

Metal-composite hybrid structures have become essential in aeronautical construction for economic and environmental reasons as maintaining good mechanical properties. Due to the different assembled materials, which present a distinctly different machinability, the parameters must change during machining to allow this optimization (Rey, 2016). In the past, the procedure for optimizing cutting parameters were time disconnected to the manufacturing process. With all the connectivity of machines, automation and networking, now-a-days in the focus of Industrial internet of things (I-Iot), the real-time identification of parameters for improving the process is an industrial reality (Wenkler *et al.*, 2018; Chen *et al.*, 2019). The political environmental protection initiatives related to aerospace industry (laws, and directives) push researchers to reduce times and costs, increase the efficiency and to develop flexible and smart processes (Cao *et al.*, 2017).

It is a fact that thousands of holes have to be drilled for assembling airplanes, so smart drilling is a key point for performance maximization. Increasing the feed rate or cutting speed on the layer that presents higher machinability is directly related to this goal (Geier *et al.*, 2019). Smart drilling is, so, the adaptation of the cutting parameters in real time, which requires the characterization and modeling of the evolution of the process variables (force, torque and power depending on the cutting feed and spindle speed), the creation and management of a database, the processing of data and real-time adjustment of the machining parameters (Klyuchnikov *et al.*, 2019; Uekita and Takaya, 2017). These models are associated with the capacity for identification, data processing and real-time action offered by machine learning tools (Sun *et al.*, 2019).

This work proposes to construct a data base for smart drilling strategies on bi-metallic stack workpiece in order to identify the material through specific force map. The drilling experiments were developed in both Aluminum and Titanium workpieces separately, using the same tool geometry. The average specific force was calculated for a wide range of cutting parameters. The identification map presents the results of the specific cutting force, calculated using the cutting power, and the specific feed force, using the feed force, in both materials.

2. SPECIFIC CUTTING FORCE AND SPECIFIC FEED FORCE

The machining force for each cutting edge is described by the vector $\vec{F}_m$ that can be decomposed on the local referential frame: F_c, the cutting force tangential to the cutting speed $\vec{V}_c$, F_f, the feed force aligned to the tool axis, and F_r on

the radial direction (Araújo *et al.*, 2020).

$$\vec{F}_m^{(1)} = \begin{bmatrix} F_c^{(1)} \\ F_r^{(1)} \\ F_f^{(1)} \end{bmatrix} \tag{1}$$

In a mechanistic model, for homogeneous material, these components are considered to be proportional to the chip cross-sectional area. This leads to the constants of proportionality called "specific force", that depend on the cutter geometry, cutting conditions, tool and workpiece material (Jayaram *et al.*, 2001). In drilling, the local specific force changes along the cutting edge as the cutting speed varies. Although, for a fixed tool dimension it is possible to calculate an average specific force considering the total chip load A_c.

Hence, the average specific cutting force K_c (MPa) for a pair tool-workpiece in drilling can be calculated using cutting force for a single cutting edge $F_c^{(1)}$ (N) as represented in Equation 2. For experimentally determining the K_c in drilling, as it is not possible to easily measure the contribution of a single edge, the cutting power P_c (W) is used considering the two tool principal cutting edges (Wenkler *et al.*, 2018).

$$K_c = \frac{F_c^{(1)}}{A_c} = \frac{120\ P_c}{V_c\ f_z\ D} \tag{2}$$

where f_z is the feed per tooth and D the nominal tool diameter.

Similarly, the specific feed force K_z (MPa) can be calculated using the feed force of a single cutting edge $F_z^{(1)}$. The total force in vertical direction F_z is a sum of the feed force from both cutting edges ($F_z = 2F_f$):

$$K_f = \frac{F_f^{(1)}}{A_c} = \frac{F_f^{(1)}}{f_z\ (D/2)} = \frac{F_z}{f_z\ D} \tag{3}$$

3. MATERIALS AND METHODS

During the experiments, power and force were measured for drilling two workpiece materials: Aluminum 2017A and Ti6Al4V titanium alloy. These experiments were done following the experimental setup and design of experiments described below. Later, the collected data was used to make power and force comparisons, as well as the identification map with the specific cutting and feed forces.

3.1 Experimental setup

All drilling experiments were developed in a CNC milling center DMU85 using flood water-based coolant internally through the drilling tool. The workpieces were fixed in a 9257B Kistler dynamometer, as shown in Figure 1(a). It is important to notice that in all cases the holes were drilled in the measuring area of the dynamometer. The force acquisition used a 5070 Kistler amplifier. For power acquisition, a Montronix power sensor PS200-DGM measured the input of effective electrical power of spindle. Analogical data from force and power is converted to digital using a 9201 National Instruments acquisition module (10 kHz acquisition rate) and the *LabView* software was used for recording data. For making the holes, solid carbide drilling tools of 11 mm diameter, coated with TiAlN and a point angle of 140^o were used (Code: WPC – VA – TiAlN 11 623 110 from Klenk/Ceratizit). Further tool dimensions are shown in Figure 1(b).

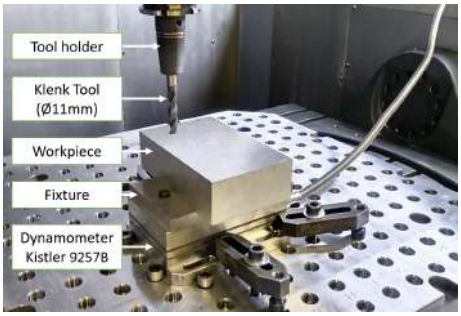

(a) Experimental elements

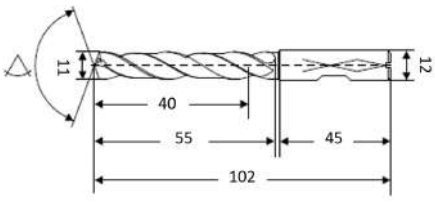

(b) Tool dimensions (*mm*) (Ceratizit, 2019)

Figura 1: Experimental setup

3.2 Design of Experiments

The range of cutting parameters is wider than usual because the goal was to compare the Aluminum and Titanium drilling results using the same data input. A full factorial design of experiments is represented by the blue points in

Figure 2: for Aluminum $V_c = 20$, 60 and 100 *m/min* and $f_z = 0.02$, 0.10 and 0.18 *mm/th* and for Titanium $V_c = 20$, 40 and 60 *m/min* and $f_z = 0.02$, 0.06 and 0.10 *mm/th*. The three red points on each work space represent the data validation points.

For all tests, the drilling length was set as 15 mm and a new tool was used every new material. Furthermore, to check if the wear influenced the results, for every three experiments made, the first ones were repeated. Those were called *check points* and were used to analyze if force and power results were maintaining in the same range as the tool has been worn.

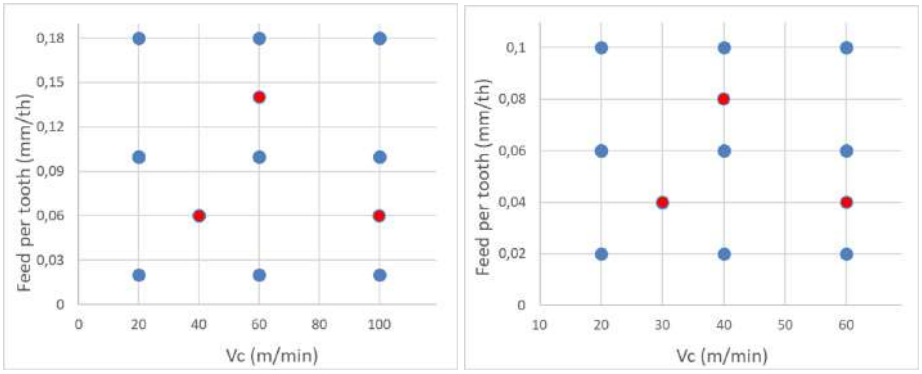

(a) Aluminum (b) Titanium

Figura 2: DOE workspace

4. EXPERIMENTAL RESULTS

The results of force, power and specific force for both materials are presented in the following subsections. The graphs are presented in terms of length of the hole and the images scales were maintained equal for both materials to allow a better comparison of results.

4.1 Feed force results

Regarding the cutting force, Figures 3 and 4 summarizes the results obtained per length of the hole for Aluminum and Titanium, respectively. Each figure contains results of different cutting speeds. Figures 3(a) and 4(a) were taken using the lower feed values and 3(c) and 4(c) the highest ones. As it can be seen, the force increases for higher feed values, while no significant variation could be observed when varying velocities.

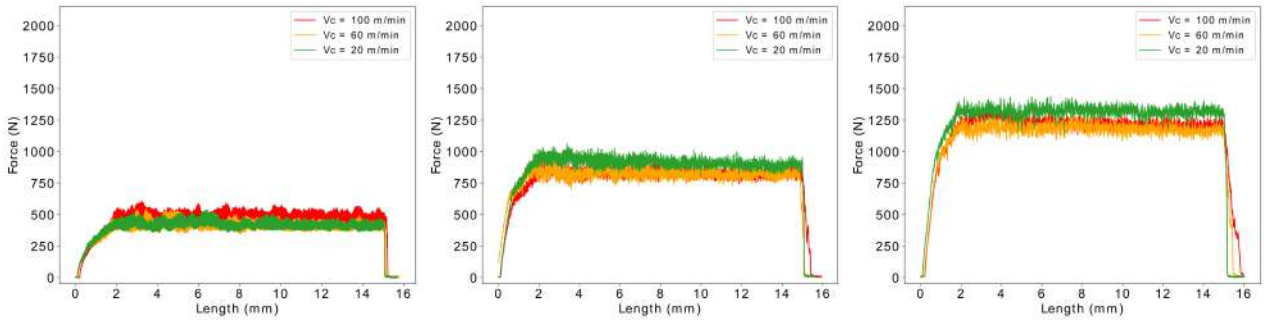

(a) $f_z = 0.02$ *mm/th* (b) $f_z = 0.10$ *mm/th* (c) $f_z = 0.18$ *mm/th*

Figura 3: Experimental feed force for drilling Aluminum

4.2 Cutting power results

Cutting power results are shown in Figures 5 and 6 for Aluminum and Titanium, respectively. Likewise, it can be observed that, for both materials, the power increases for higher feed values and higher cutting speeds.

From the results presented in Figure 6, it can be noticed that the cutting power on Titanium showed an increasing behavior during the cutting process. This behavior is associated to the elastic recovery of the cylindrical surface on Ti6Al4V as reported in the work of Shugurov *et al.* (2020) where the lamellar and bimodal microstructures were subjected to nanocratch test. In their studies, they found out that the elastic recovery for Titanium varied from 9% to 15%, being larger for bi-modal microstructures due to the elastic deformation of the samples and the development of reversible $\beta \rightarrow \alpha \rightarrow \beta$ phase transformation, which is related to the presence of vanadium in the crystal lattice, that leads to a higher elastic recovery. Shugurov *et al.* (2020) also addressed the influence of the material microstructure and elastic

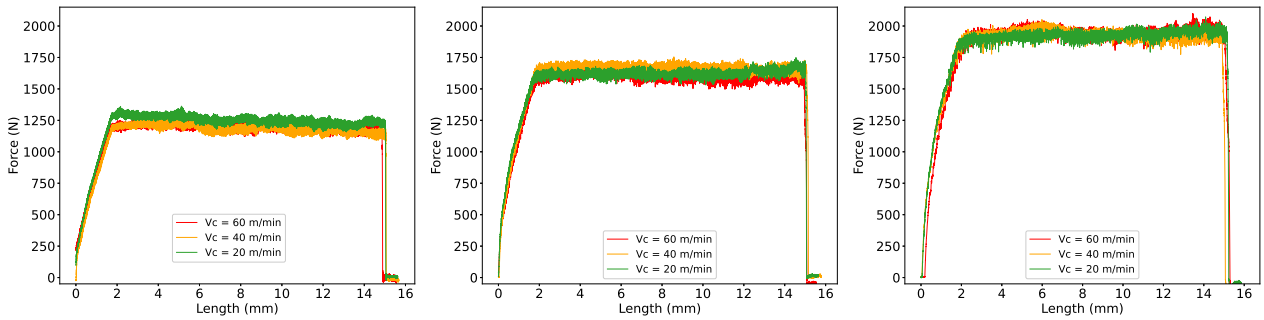

(a) $f_z = 0.02$ *mm/th* (b) $f_z = 0.06$ *mm/th* (c) $f_z = 0.10$ *mm/th*

Figura 4: Experimental feed force for drilling Titanium

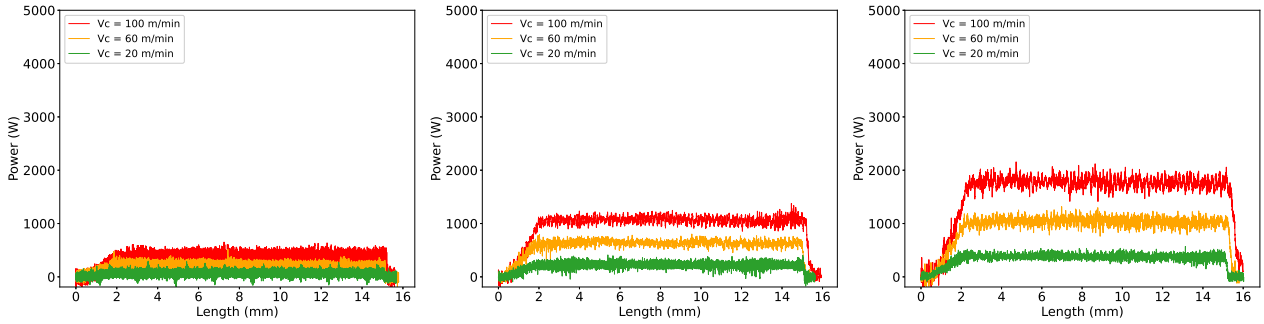

(a) $f_z = 0.02$ *mm/th* (b) $f_z = 0.10$ *mm/th* (c) $f_z = 0.18$ *mm/th*

Figura 5: Experimental cutting power for drilling Aluminum

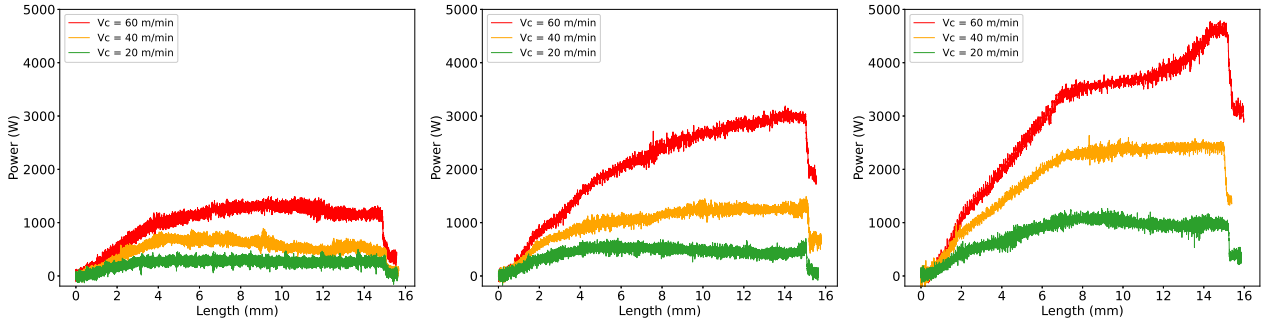

(a) $f_z = 0.02$ *mm/th* (b) $f_z = 0.06$ *mm/th* (c) $f_z = 0.10$ *mm/th*

Figura 6: Experimental cutting power for drilling Titanium

recovery on the ploughing mechanisms, which is the main mechanism of abrasive wear. Taking this into consideration, the elastic recovery of the material during cutting leads to an increase in power, which can drive the tool to a higher abrasive wear. This behavior was not present in Aluminum data.

4.3 Specific cutting and feed forces

Figures 7(a) and 7(b) shows an comparison of the specific cutting force (K_c) behavior when drilling Aluminum and Titanium, respectively. Figures 7(c) and 7(d) shows the same comparison, but for the specific feed force (K_f). As it can be seen, K_c and K_f values are higher for lower feed rates, as for its calculation power and force, respectively, are divided by feed. In addition, the results are higher for drilling titanium, due to its poor machinability caused by its higher hardness and higher yield and tensile strengths.

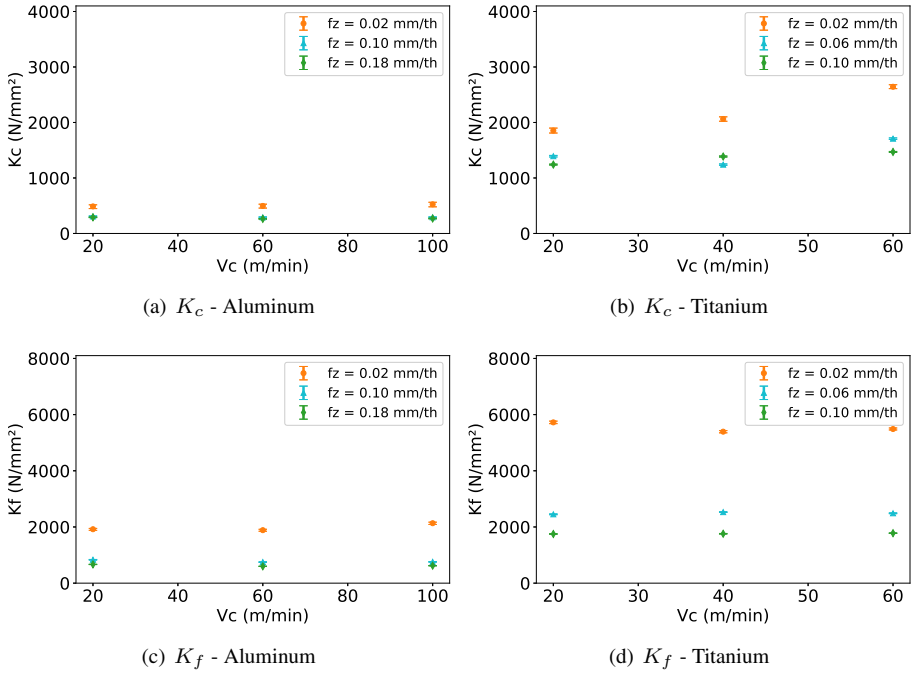

(a) K_c - Aluminum (b) K_c - Titanium

(c) K_f - Aluminum (d) K_f - Titanium

Figura 7: Average K_c and K_f per experiment with different cutting speeds during drilling

5. IDENTIFICATION MAP

The K_c and K_f variation with feed is shown in Figure 8(a) and 8(b), where comparisons between both materials are made. The behavior of results are similar, considering that the results for titanium are higher. Another comparison is presented in Figure 8(c), where an identification map of K_c per K_f is shown. From there, it can be noticed that there is a clear distinction in the range of force and power results for drilling Titanium and Aluminum.

This gap between materials makes it suitable for applying smart drilling techniques in the drilling process of stacks materials made out of Aluminum and Titanium. Since the identification map obtained in Figure 8(c) allows the distinction between these materials from its power and force data, considering cutting speed, feed and tool diameter used, when a stack is being drilled, it is possible to adjust the cutting parameters in real time to make the drilling process more efficient.

Assuming a situation where the estimated K_c values are lower than 1000 N/mm^2 (for parameters range used in this work), the material drilled is presumed to be aluminum and the cutting speed can be raised to achieve better drilling results and the process become less time consuming. On the other side, if the values are too high, the material being drilled should be titanium and the velocity shall be reduced to meet the recommended parameters. Although, the region where the titanium meets aluminum or vice versa is a critical area, because the tool is cutting both materials at the same time. When this change occurs, there is a increasing/decreasing power region that can be used as a trigger to adjust the cutting speed. This alteration should be made as soon as the change in material is detect to reduce tool damage, specially when the change is from aluminum to titanium.

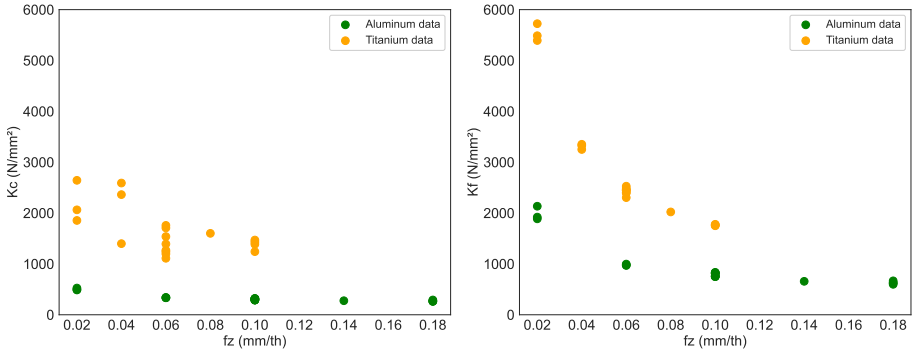

(a) K_c (b) K_f

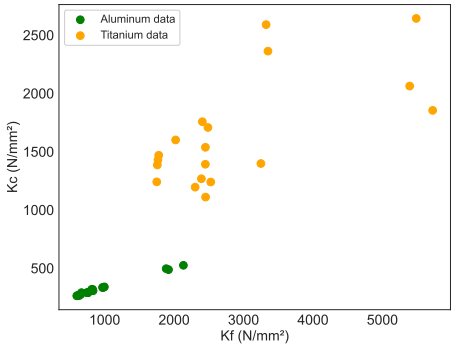

(c) K_c and K_f

Figura 8: Identification map with K_c per K_f for both materials

6. CONCLUSIONS

This article focused on the analysis of force and power during drilling Titanium and Aluminum workpieces aiming the identification of each material during cutting. As expected, the specific cutting and feed force were higher for titanium, due to its material poor machinability, which allows clearly the distinction between both material. The results shows that the methodology can be used as a smart drilling technique for the detection of the drilled material using monitoring data.

One important point observed in the signal pattern is that: during machining Titanium the elastic recovery of material leads to an increase in power when the tool penetrates the workpiece. This elastic recovery disturbs the identification, it could induce to a wrong interpretation that the specific cutting force is increasing inside the hole, which it is not the case. A second point to note is that when the tool wear plays a role, the values of specific forces of Aluminum could cross the area of the Titanium region as these values will tend to rise. Although, in this experiments, no significant tool wear was observed, in a large scale process this phenomena has to be taken into account.

7. ACKNOWLEDGMENTS

This article received financial support from projet européen RODEO (program H2020-CleanSky2) managed by Université Paul Sabatier (UPS) and also supported by project Jeunes Chercheurs 2020 by Institut National des Sciences Appliquées de Toulouse (INSA) for the mobility and expenses of the first author on her internacional mobility in laboratory Institut Clément Ader (ICA), France. The authors thank also the National Council for Scientific and Technological Development (CNPq) and Universidade de São Paulo for the local support during her Master thesis in Brazil.

8. REFERENCES

Araújo, A.C., Landon, Y. and Lagarrigue, P., 2020. "Smart drilling for aerospace industry: state of art in research and education". *14th CIRP Conference on Intelligent Computation in Manufacturing Engineering*.

Cao, H., Zhang, H. and Chen, X., 2017. "The concept and progress of intelligent spindles: A review". *International Journal of Machine Tools and Manufacture*, pp. 21–52.

Ceratizit, 2019. "Catalogue ceratizit". `https://cuttingtools.ceratizit.com/gb/en/download/catalogue.html`. Access: 2020-11-10.

Chen, J., Hu, P., Zhou, H., Yang, J., Xie, J., Jiang, Y., Gao, Z. and Zhang, C., 2019. "Toward intelligent machine tool". *Engineering*, pp. 679–690.

Geier, N., Davim, P. and Szalay, T., 2019. "Advanced cutting tools and technologies for drilling carbon fibre reinforced polymer (cfrp) composites: A review". *Composites Part A: Applied Science and Manufacturing*.

Jayaram, S., Kapoor, S.G. and DeVor, R.E., 2001. "Estimation of the specific cutting pressures for mechanistic cutting force models". *International Journal of Machine Tools and Manufacture*, p. 265–281.

Klyuchnikov, N., Zaytsev, A., Gruzdev, A., Ovchinnikov, G., Antipova, K., Ismailova, L., Muravleva, E., Burnaev, E., Semenikhin, A., Cherepanov, A., Koryabkin, V., Simon, I., Tsurgan, A., FedorKrasnov and Koroteev, D., 2019. "Data-driven model for the identification of the rock type at a drilling bit". *Journal of Petroleum Science and Engineering*, pp. 506–516.

Rey, P.A., 2016. *Characterization and optimization of the orbital drilling of Ti6Al4V and CFRP / Ti6Al4V stacks*. Ph.D. thesis, the University of Toulouse, Toulouse. Tese de doutorado.

Shugurov, A., Panin, A., Dmitriev, A. and Nikonov, A., 2020. "Recovery of scratch grooves in ti-6al-4v alloy caused by reversible phase transformations". *Metals*.

Sun, J., Li, Q., Chen, M., Ren, L., Huang, G., Li, C. and Zhang, Z., 2019. "Optimization of models for a rapid identification of lithology while drilling - a win-win strategy based on machine learning". *Journal of Petroleum Science and Engineering*, pp. 321–341.

Uekita, M. and Takaya, Y., 2017. "Tool condition monitoring technique for deep-hole drilling of large components based on chatter identification in time – frequency domain". *Measurement*, pp. 199–207.

Wenkler, E., Arnold, F., Hänel, A., Nestler, A. and Brosius, A., 2018. "Intelligent characteristic value determination for cutting processes based on machine learning". *12th CIRP Conference on Intelligent Computation in Manufacturing Engineering*.

9. INFORMATION'S RESPONSIBILITY

The authors are responsible for the information included in this work.